The origin and spread of locally adaptive seasonal camouflage in snowshoe hares
— Source link ☒

Matthew R. Jones, L. Scott Mills, Jeffrey D. Jensen, Jeffrey M. Good

Institutions: Arizona State University, University of Montana

Related papers:

- The evolutionary pathways for local adaptation in mountain hares

- The evolutionary history of Nebraska deer mice: local adaptation in the face of strong gene flow

- Broad geographic sampling reveals predictable, pervasive, and strong seasonal adaptation in Drosophila

- Broad geographic sampling reveals predictable and pervasive seasonal adaptation in Drosophila

- Adaptive Introgression Promotes Fast Adaptation In Oaks Marginal Populations

1   **The origin and spread of locally adaptive seasonal camouflage in snowshoe hares**

2   Matthew R. Jones[1,2], L. Scott Mills[3,4], Jeffrey D. Jensen[2], Jeffrey M. Good[1,3]

3   [1]Division of Biological Sciences, University of Montana, Missoula, MT 59812, USA.

4   [2]School of Life Sciences, Arizona State University, Tempe, AZ 85281, USA

5   [3]Wildlife Biology Program, University of Montana, Missoula, MT 59812, USA.

6   [4]Office of Research and Creative Scholarship, University of Montana, Missoula, MT 59812,

7   USA.

8   Corresponding authors: matthew.r.jones.1@asu.edu, jeffrey.good@umontana.edu

9   **Abstract**

10   Adaptation is central to population persistence in the face of environmental change, yet we rarely

11   precisely understand the origin and spread of adaptive variation in natural populations. Snowshoe

12   hares (*Lepus americanus*) along the Pacific Northwest (PNW) coast have evolved brown winter

13   camouflage through positive selection on recessive variation at the *Agouti* pigmentation gene

14   introgressed from black-tailed jackrabbits (*L. californicus*). Here we combine new and published

15   whole genome and exome sequences with targeted genotyping of *Agouti* in order to investigate

16   the evolutionary history of local seasonal camouflage adaptation in the PNW. We find evidence

17   of significantly elevated inbreeding and mutational load in coastal winter-brown hares, consistent

18   with a recent range expansion into temperate coastal environments that incurred indirect fitness

19   costs. The genome-wide distribution of introgression tract lengths supports a pulse of

20   hybridization near the end of the last glacial maximum, which may have facilitated range

21   expansion via introgression of winter-brown camouflage variation. However, signatures of a

22   selective sweep at *Agouti* indicate a much more recent spread of winter-brown camouflage.

23   Through simulations we show that the temporal lag between the hybrid origin and subsequent

24   selective sweep of the recessive winter-brown allele can be largely attributed to the limits of

25   natural selection imposed by simple allelic dominance. We argue that while hybridization during

26   periods of environmental change may provide a critical reservoir of adaptive variation at range

27   edges, the probability and pace of local adaptation will strongly depend on population

28   demography and the genetic architecture of introgressed variation.

Introduction

29

30   Local adaptation is fundamental to the persistence of populations during periods of rapid

31 environmental change. In particular, local adaption to marginal habitats may increase a species'

32 niche breadth and range size (Holt and Gomulkiewicz 1997), enhancing their evolutionary

33 resilience (Sgrò et al. 2011; Slatyer et al. 2013; Forsman 2016; Mills et al. 2018). Consequently,

34 range edges where populations encounter marginal habitats and less favorable conditions may

35 harbor crucial adaptive variation that facilitates long-term persistence in the face of

36 environmental change (Hampe and Petit 2005; Hill et al. 2011; Cheng et al. 2014). Yet, range

37 boundaries may also reflect the limits of natural selection if they are defined by environments

38 where populations have failed to adapt (Antonovics 1976; Kirkpatrick and Barton 1997; Bridle

39 and Vines 2007). Revealing how adaptive variation arises and spreads along range edges is,

40 therefore, fundamental to understand the limitations of adaptation to new or changing

41 environments (Ackerly 2003; Hampe and Petit 2005). However, we rarely possess detailed

42 knowledge of the genetic basis and history of local adaptation in natural populations.

43   Several decades of theoretical research have established a framework for predicting

44 demographic conditions along range margins, which are crucial in shaping population-level

45 fitness and the potential for adaptation and range expansion. Populations inhabiting marginal

46 habitats are generally predicted to be small and occur at low densities (Antonovics 1976;

47 Kirkpatrick and Barton 1997), resulting in relatively reduced rates of beneficial mutation and

48 levels of standing genetic variation (Pfennig et al. 2016). Small range-edge populations may

49 further experience higher rates of inbreeding due to genetic drift (Wright 1931; Barton 2001) and

50 accumulate deleterious variation (i.e., mutational load; Lynch et al. 1995; Willi et al. 2018),

51 which can decrease the probability of population persistence (Mills and Smouse 1994). Elevated

52   individual inbreeding and mutational load along range edges may also reflect past histories of

53   adaptation and range expansion that result in non-equilibrium population dynamics. For instance,

54   mating between close relatives may increase in founder populations that have recently undergone

55   severe population contractions associated with range expansions (Frankham 1998). Likewise,

56   mutational load may be amplified through the colonization of new environments because

57   population contractions reduce the efficacy of selection against deleterious alleles at the

58   expansion front (i.e., expansion load; Peischl et al. 2013; Henn et al. 2016; González-Martínez et

59   al. 2017; Willi et al. 2018). Thus, when adaptation does occur along range margins it may

60   produce negative feedbacks on population fitness and evolutionary potential.

61   Patterns of migration into range edge populations are also pivotal to their fitness and

62   adaptive potential. Larger core populations are expected to produce relatively more migrants

63   than smaller edge populations, leading to asymmetric rates of gene flow between core and

64   peripheral habitats. In extreme scenarios, edge populations with low population growth rates

65   ($\lambda<1$) can be demographic sinks that are maintained by immigration from the core of the range

66   (Holt and Gomulkiewicz 1997; Griffin and Mills 2009). Highly asymmetric gene flow may

67   further reduce fitness and hinder adaptation along the range edge by continually swamping local

68   selection (Haldane 1930; Garcia-Ramos and Kirkpatrick 1997; Kirkpatrick and Barton 1997;

69   Kawecki 2008). However, gene flow from core populations into edge populations may ultimately

70   promote adaptive responses when edge populations are small and ecological gradients are

71   shallow (Polechová 2018; Bontrager and Angert 2019). Hybridization between species may also

72   facilitate adaptation and range expansion if edge populations intersect with the range of closely-

73   related species that are adapted to local habitats (Baker 1948; Lewontin and Birch 1966; Burke

74   and Arnold 2001; Rieseberg et al. 2007; Kawecki 2008; Pfennig et al. 2016). Introgression may

75   provide a crucial source of large-effect variation (Hedrick 2013), which is predicted to be scarce

76   in small populations but often necessary for range-edge adaptation and expansion (Behrman and

77   Kirkpatrick 2011; Gilbert and Whitlock 2016). Putative adaptive introgression has now been

78   shown in numerous species (e.g., Song et al. 2011; Pardo-Diaz et al. 2012; Huerta-Sánchez et al.

79   2014; Lamichhaney et al. 2015; Miao et al. 2016; Jones et al. 2018; Oziolor et al. 2019) and has

80   been specifically linked to range expansions in Australian fruit flies (Lewontin and Birch 1966),

81   sunflowers (Rieseberg et al. 2007), and mosquitoes (Besansky et al. 2003). While hybridization

82   may facilitate adaptation and range expansion via large-effect mutations (Hedrick 2013; Nelson

83   et al. 2019), the factors influencing the pace of adaptive introgression are often unclear.

84   Snowshoe hares (*Lepus americanus*) are broadly distributed across boreal and montane

85   forests of North America. Most populations of hares undergo seasonal molts between brown

86   (summer) and white (winter) coats to maintain crypsis in snow-covered environments. Seasonal

87   camouflage is a crucial component of fitness in this system (Mills et al. 2013) as hares that

88   become mismatched with their environment experience dramatically increased predation rates

89   (i.e., 3-7% increase in weekly survival mortality; Zimova et al. 2016). However, some hares have

90   adapted to mild winter environments by remaining brown in the winter (Mills et al. 2018).

91   Brown winter camouflage in snowshoe hares is relatively rare across the entire range (<5% of

92   the range), but predominant along portions of the southern range edge in the Pacific Northwest

93   (PNW; Nagorsen 1983) with occurrence closely tracking regions of low seasonal snow cover

94   (Mills et al. 2018). As snow cover across North America continues to decline under climate

95   change, it is predicted that winter-brown camouflage may spread from the edge to the interior of

96   the range, enhancing the evolutionary resilience of snowshoe hares (Jones et al. 2018; Mills et al.

97   2018). We previously demonstrated that brown versus white winter camouflage in PNW

4

98   snowshoe hares is determined by a simple *cis*-regulatory polymorphism of the *Agouti*

99   pigmentation gene that influences its expression during the autumn molt (Jones et al. 2018). The

100   locally adaptive winter-brown allele is fully recessive and derived from introgressive

101   hybridization with black-tailed jackrabbits (*Lepus californicus*), a closely-related scrub-grassland

102   species that remains brown in the winter (Jones et al. 2018). Thus, the evolution of brown winter

103   coats along coastal environments in the PNW represents one of the few verified cases of

104   introgression underlying an adaptive trait of known ecological relevance in mammals (Taylor

105   and Larson 2019).

106   The establishment of this genotype-to-phenotype link provides a powerful opportunity to

107   examine how population history and hybridization shape local adaptation and expansion along

108   the range edge. Here we seek to deepen our understanding of 1) the population history of PNW

109   range edge snowshoe hares and 2) the origin and spread of winter-brown camouflage across

110   coastal PNW environments. We first use previously published targeted exome data (61.7 Mb for

111   80 individuals; Jones et al. 2018) to estimate historical changes in population size (N), individual

112   inbreeding coefficients, and mutational load in PNW hares. We then combine 11 whole genome

113   sequences (WGS; six new and five previously published) with 61 newly assembled complete

114   mitochondrial genomes and targeted genotyping of the introgressed *Agouti* region across 106

115   hares to resolve the timing of hybridization with black-tailed jackrabbits and the subsequent

116   spread of winter-brown coat color variation. We use these data to test theoretical predictions for

117   the maintenance and spread of adaptive variation in peripheral environments. Our study provides

118   rare empirical insight into the dynamic interplay of environmental change, hybridization, and

119   selection along range-edge environments and its evolutionary consequences.

120

Methods

<u>Genomic data generation</u>

All sample collection with live animals was performed under approved state permits and associated Animal Use Protocols approved through the University of Montana Institutional Animal Care and Use Committee (IACUC).

For some analyses, we used previously generated targeted whole exome data (61.7-Mb spanning 213,164 intervals; ~25-Mb protein-coding exons, ~28-Mb untranslated region, ~9-Mb intronic or intergenic) for 80 snowshoe hares (21× mean coverage) collected from Washington (WA; n=13 winter-brown, n=13 winter-white), Oregon (OR; n=13 winter-brown, n=13 winter-white), Montana (MT; n=14 winter-white), and southwest British Columbia (BC; n=14 winter-brown; Jones et al. 2018). Hares from OR and WA were collected in the Cascade Range where populations are polymorphic for winter coat color (Fig. 1A). Hares from Seeley Lake in western MT are winter-white individuals, while those from BC were collected in low-lying regions near the Pacific coast where snowshoe hares are all winter-brown (Fig. 1A). To infer the history of hybridization, we performed whole genome resequencing of three black-tailed jackrabbits from OR and California (CA) and two winter-brown snowshoe hares from OR and BC. These samples complement WGS data previously generated for two black-tailed jackrabbits from Nevada (NV; one of which was sequenced to higher coverage in this study) and snowshoe hares from MT, WA, Utah (UT), and Pennsylvania (PA; Jones et al. 2018). We extracted genomic DNA following the Qiagen DNeasy Blood and Tissue kit protocol (Qiagen, Valencia, CA) and prepared genomic libraries following the KAPA Hyper prep kit manufacturer's protocol. For all libraries, we sheared genomic DNA using a Covaris E220evolution ultrasonicator and performed a stringent size selection using a custom-prepared carboxyl-coated magnetic bead mix (Rohland

6

144   and Reich 2012) to obtain average genomic fragment sizes of 400-500 bp. We determined

145   indexing PCR cycle number for each library with quantitative PCR (qPCR) on a Stratagene

146   Mx3000P thermocycler (Applied Biosystems) using a DyNAmo Flash SYBR Green qPCR kit

147   (Thermo Fisher Scientific). Final libraries were size-selected again with carboxyl-coated

148   magnetic beads, quantified with a Qubit (Thermo Fisher Scientific), and pooled for sequencing

149   by Novogene (Novogene Corporation Ltd.; Davis, CA) on two lanes of Illumina HiSeq4000

150   using paired-end 150 bp reads.

151   To resolve the history of selection on the winter-brown *Agouti* allele, we performed

152   targeted enrichment and sequencing to genotype 106 hares at the *Agouti* locus (*n*=37 WA, *n*=64

153   OR, *n*=5 MT). We developed a custom set of IDT xGen Lockdown probes spanning a 596.4 kb

154   interval centered on the *Agouti* gene and extending to flanking regions (chromosome

155   4:5,250,800-5,847,200; coordinates based on the European rabbit (*Oryctolagus cuniculus*)

156   oryCun2 genome build). The probe sequences were based on a snowshoe hare pseudoreference

157   genome (~33×; Jones et al. 2018) derived from iterative mapping to the rabbit genome (Carneiro

158   et al. 2014). We targeted 96 uniquely-mapped 100 bp regions (based on low coverage WGS data

159   from Jones et al. (2018)) that contained one or more diagnostic SNPs for winter coat color,

160   allowing us to infer winter coat color for samples based on their *Agouti* genotype. We prepared

161   genomic libraries for targeted *Agouti* sequencing following a modified version of Meyer and

162   Kircher (2010), as described in Jones et al. (2018). We performed hybridization reactions on 500

163   ng of pooled libraries (10-16 individual libraries per pool), 5 μg of custom prepared snowshoe

164   hare C_0t-1 DNA, and 2 nM of blocking oligos. Washing and recovery of captured DNA was

165   performed following the IDT xGen Lockdown probe hybridization capture protocol (version 2).

166   Each capture library was then amplified in 50 μl reactions with 1X Herculase II reaction buffer,

167   250 μM each dNTP, 0.5 μM each primer, 1 μl Herculase II fusion polymerase, and 20 μl library

168   template. The PCR temperature profile consisted of a 45 second 98°C denaturation step,

169   followed by 24 cycles of 98°C for 15 seconds, 60°C for 30 seconds, and 72°C for 30 seconds,

170   with a final 72°C elongation step for 1 minute. We cleaned and size-selected final libraries with

171   1.2X carboxyl-coated magnetic beads and verified target enrichment with qPCR. *Agouti* capture

172   libraries were then pooled and sequenced with other libraries across two lanes of Illumina

173   HiSeq4000 at the University of Oregon Core (Eugene, OR) and Novogene.

174

175   Read processing and variant calling

176   For all raw sequence data, we trimmed adapters and low-quality bases (mean phred-scaled

177   quality score <15 across 4 bp window) and removed reads shorter than 50 base pairs (bp) using

178   Trimmomatic v0.35 (Bolger et al. 2014). We then merged paired-end reads overlapping more

179   than 10 bp and with less than 10% mismatched bases using FLASH2 (Magoč and Salzberg

180   2011). Cleaned exome and *Agouti* capture reads were mapped using default settings in BWA-

181   MEM v0.7.12 (Li 2013) to the snowshoe hare pseudoreference genome. WGS data were mapped

182   to either the snowshoe hare or a black-tailed jackrabbit pseudoreference, which was also created

183   by iteratively mapping to the rabbit genome (Jones et al. 2018). We used *PicardTools* to remove

184   duplicate reads with the MarkDuplicates function and assigned read group information with the

185   AddOrReplaceReadGroups function. Using GATK v3.4.046 (McKenna et al. 2010), we

186   identified poorly aligned genomic regions with RealignerTargetCreator and performed local

187   realignments with IndelRealigner. We performed population-level multi-sample variant calling

188   using default settings with the GATK UnifiedGenotyper and filtered variants in VCFtools

189   v0.1.14 (Danecek et al. 2011). For whole exome and whole genome data, we filtered genotypes

8

190   with individual coverage <5× or >70× or with a phred-scaled quality score <30. Additionally, we

191   removed all indel variants and filtered single nucleotide polymorphisms (SNPs) with a phred-

192   scaled quality score <30 and Hardy-Weinberg P<0.001. We required that sites have no missing

193   data across individuals. For targeted *Agouti* SNP data, we additionally filtered heterozygous

194   genotypes with allelic depth ratios >3 and sites with > 50% missing data across individuals. We

195   phased haplotypes and imputed missing data with Beagle v4.1 (Browning and Browning 2007)

196   and used *Haplostrips* (Marnetto and Huerta-Sánchez 2017) to visualize haplotype structure.

197

198   Population size history and inbreeding coefficients of PNW hares

199   We used the program ∂a∂i (Gutenkunst et al. 2009) to infer historical population size (N)

200   changes in PNW snowshoe hare populations (BC, MT, OR, and WA) using the folded site

201   frequency spectrum (SFS) of synonymous variants from our extensive whole exome data set. We

202   used the folded SFS to be consistent with statistical inferences of the distribution of fitness

203   effects (see below). For each population, we tested a standard neutral equilibrium model, a two-

204   epoch model (single instantaneous N change), a three-epoch model (two instantaneous N

205   changes), an exponential N growth model, and an instantaneous N change + exponential N

206   growth model. We inferred values for parameters ν, the population size relative to ancestral N

207   (N_{anc}; e.g., ν=1 if N=N_{anc}) and t, the time of population size changes in units of $2N_{anc}$

208   generations. We performed 100 independent runs under each model starting with parameter

209   values sampled randomly across a uniform distribution ($0.001 < \nu < 100$, $0 < 2N_e t < 2$). For each

210   model, we selected parameters with the highest log-likelihood value and chose the overall best

211   model using a composite-likelihood ratio test with the Godambe Information Matrix (Coffman et

212   al. 2016). We further checked the validity of maximum likelihood models by comparing the

9

213 predicted SFS to the observed SFS for each population (Fig. S2). We determined 95%

214 confidence intervals for parameter estimates using the Godambe Information Matrix with 100

215 bootstrap data sets comprised of one randomly selected synonymous SNP per 10 kb.

216   SFS-based approaches are often underpowered or inappropriate for inferring recent

217 population size changes (Robinson et al. 2014; Beichman et al. 2018). For instance, even with a

218 sufficient sample size, a historically large population that has very recently contracted in size

219 (i.e., not in equilibrium) may nonetheless have a large variance N_e. However, individuals in such

220 populations may exhibit elevated individual inbreeding coefficients (F_{IS}), calculated as $1-H_o/H_e$

221 where H_o is the observed heterozygosity and H_e is expected heterozygosity assuming random

222 mating. To examine evidence for recent population contractions, we calculated the mean of the

223 individual inbreeding coefficient (F_{IS}) for each population using VCFtools and tested for

224 significant differences between populations with a two-tailed Student's t-Tests in R (R Core

225 Team 2018).

226

227 <u>Mutational load and the distribution of fitness effects</u>

228 For each PNW population, we measured the proportion of homozygosity across SNPs with

229 predicted phenotypic effects (nonsynonymous and nonsense) as an indicator for relative

230 differences in mutational load under a recessive deleterious mutation model (González-Martínez

231 et al. 2017). We tested for significant differences in the proportion of homozygosity across

232 populations using two-sided Z-tests for proportions in R (R Core Team 2018). Additionally, we

233 used whole exome data to infer the distribution of selection coefficients of segregating variation,

234 more commonly referred to as the distribution of fitness effects (DFE). In principle, we can infer

235 the DFE from the SFS of selected sites because neutral, weakly deleterious, and strongly

10

236   deleterious variation should segregate at different frequencies in populations (Keightley and

237   Eyre-Walker 2010). The DFE of segregating variation is commonly inferred by first fitting a

238   population history model to the SFS of neutral sites (often synonymous SNPs) and then fitting a

239   mutational model to the SFS of selected sites (often nonsynonymous SNPs), while controlling

240   for the effect of population history (i.e., changes in N) on the SFS of selected sites (Keightley

241   and Eyre-Walker 2010). Here we implement this approach using the *Fit∂a∂i* module (Kim et al.

242   2017). We used the maximum likelihood parameter values from our inferred demographic model

243   to control for population history and fit a simple DFE to the folded SFS of nonsynonymous

244   variants (identified with SNPeff; Cingolani et al. 2012) described by a gamma distribution of

245   selective effects with a shape (α) and scale (β) parameter. To estimate variance in shape and

246   scale parameters, we used 100 bootstrap datasets randomly sampling 50% of nonsynonymous

247   sites and performed 10 independent runs on each dataset. We used random starting values

248   between 0.001 and 1 for the shape parameter and values between 0.01 and 200,000 for the scale

249   parameter. To scale the DFE from relative selection coefficients ($2N_{anc}s$) to absolute selection

250   coefficients (s), we divided the scale parameter by $2N_{anc}$ (Kim et al. 2017).

251

252   <u>The timing of hybridization</u>

253   If hybridization between snowshoe hares and black-tailed jackrabbits is rare, then the age of

254   hybridization may also reflect the age of *Agouti* introgression. We used two complementary

255   approaches to estimate the timing of hybridization between PNW snowshoe hares and black-

256   tailed jackrabbits. Previous phylogenetic analysis of partial cytochrome *b* sequences revealed

257   that some PNW snowshoe hares carry introgressed mitochondrial DNA (mtDNA) genomes

258   derived from hybridization with black-tailed jackrabbits (Cheng et al. 2014; Melo-Ferreira et al.

11

259   2014). We estimated the age of mtDNA introgression using complete mtDNA genomes for

260   snowshoe hares (*n*=56) and black-tailed jackrabbits (*n*=5) that we assembled *de novo* from newly

261   and previously generated WGS data (Jones et al. 2018) with the program NOVOPlasty

262   (Dierckxsens et al. 2017). We aligned individual mtDNA assemblies, including the rabbit

263   mtDNA reference as an outgroup (total assembled length= 16,251 bp), using default settings in

264   Clustal W v2.1 (Larkin et al. 2007) and visually verified alignment quality. We then estimated a

265   maximum clade credibility tree and node ages with a Calibrated Yule model in BEAST 2

266   (Bouckaert et al. 2014), assuming a strict molecular clock and an HKY substitution model using

267   empirical base frequencies. We specified default priors for the kappa and gamma shape

268   parameters and used a gamma distribution (alpha=0.001, beta=1000) as a prior for the clock rate

269   and birth rate parameter. We ran the MCMC for 5 million steps and calibrated divergence times

270   using a log-normal distribution for the rabbit-*Lepus* node age with a median of 11.8 million

271   generations (95% prior density: 9.8–14.3; Matthee et al. 2004).

272   We also examined patterns of autosomal introgression tracts to infer the age of nuclear

273   admixture. Given that mtDNA admixture may have been relatively ancient (Melo-Ferreira et al.

274   2014), admixture dating approaches based on linkage disequilibrium (LD) may have low power

275   due to erosion of LD through ongoing recombination (Loh et al. 2013). Therefore, we developed

276   an approach to fit the distribution of empirically inferred introgression tract lengths to tract

277   lengths simulated under various models of admixture. We first identified genome-wide tracts of

278   introgression using the program PhylonetHMM (Liu et al. 2014), which assigns one of two

279   parent trees (species tree or hybridization tree) to each variable position using a hidden Markov

280   model. PhylonetHMM robustly distinguishes between incomplete lineage sorting (ILS) and

281   introgression by allowing for switches between gene trees within each parent tree (Liu et al.

12

282   2014; Schumer et al. 2016). Alignments of WGS data for the phylogenetic analysis included two

283   black-tailed jackrabbits sampled from CA (BTJR1) and NV (BTJR2), a UT snowshoe hare

284   (previously shown as non-admixed; Jones et al. 2018), and a winter-brown WA snowshoe hare to

285   represent the admixed PNW snowshoe hare population. Here, the species tree is defined as

286   ((WA,UT),(BTJR1, BTJR2)) and the hybridization tree is defined as (UT,(WA,BTJR1/BTJR2)).

287   We specified base frequencies and transmission/transversion rates based on analysis with

288   RAxML. We identified introgression tracts as contiguous regions of the genome with an average

289   hybridization tree probability >95% across 25 variant windows (1 variant step) and excluded

290   introgression tracts shorter than 10-kb (Schumer et al. 2016). We then used the program SELAM

291   (Corbett-Detig and Jones 2016) to simulate a single pulse of admixture (lasting either 1

292   generation or 100 generations) occurring at a frequency of 0.01%, 0.1%, or 1% and recorded

293   introgression tracts >10kb every 1000 generations for 50,000 generations across 21 autosomes.

294   We performed a goodness of fit test between empirical and simulated tract length distributions

295   using Kolmogorov-Smirnov tests (K-S tests), which measure differences in the cumulative

296   fraction of data across the range of observed values (Massey 1951). To estimate the variance in

297   hybridization timing, we performed K-S tests on 100 bootstrap data sets generated by

298   subsampling 30% of the genome-wide introgression tracts.

299

300   The time to most recent common ancestor of the winter-brown haplotype

301   To understand the history of the spread of winter brown camouflage, we used targeted *Agouti*

302   SNPs to estimate the time to most recent common ancestor (TMRCA) for the winter-brown

303   *Agouti* haplotype in OR (*n*=47 individuals) and WA (*n*=35 individuals). We estimated the

304   TMRCA using a Markov chain Monte Carlo approach implemented in *startmrca* (Smith et al.

13

305   2018), which leverages information on the length distribution of the fixed selected haplotype and

306   the accumulation of derived mutations. We assumed a constant recombination rate of 1 cM/Mb

307   (Carneiro et al. 2011) and tested an upper and lower estimate for mutation rate in European

308   rabbit (2.02×10^{-9} and 2.35×10^{-9} mutations/site/generation; Carneiro et al. 2012). We also

309   explored the influence of using a divergent population (homozygous winter-white individuals

310   from MT; n=5 individuals) or a local population (homozygous winter-white individuals from OR

311   and WA; n=19 individuals) to represent the ancestral winter-white haplotype (Smith et al. 2018).

312   We assumed chr4:5480355 (in oryCun2 coordinates) as the site of the "selected allele", which

313   lies in the center of the association interval between two strong candidate insertion-deletion

314   mutations in the 5' *cis*-regulatory region of *Agouti* and is perfectly correlated with winter coat

315   color (Jones et al. 2018). We performed 100,000 iterations with a standard deviation of 20 for the

316   proposal distribution and used the final 10,000 iterations to generate posterior TMRCA

317   distributions (Smith et al. 2018).

318

319   Simulations of selection on a recessive beneficial allele

320   Assuming fixation of a single haplotype, the above framework for inferring the TMRCA should

321   reflect the age at which the beneficial haplotype began to increase rapidly in frequency (Smith et

322   al. 2018), which under some conditions may be much more recent than the age of the beneficial

323   mutation itself (Teshima and Przeworski 2006; Kelley 2012). For instance, the masking of

324   recessive alleles to selection at low frequency is expected to decrease the rate at which they

325   begin to increase in frequency, conditional on fixation (Teshima and Przeworski 2006),

326   potentially resulting in a temporal lag between a fixed allele's origin and TMRCA. However,

327   such a scenario may be unlikely as the masking of rare recessive alleles is also expected to

14

328   decrease their fixation probability (i.e., 'Haldane's sieve', Haldane 1924; Turner 1981).

329   Alternatively, an environmental change could favor a previously neutral or deleterious variant,

330   resulting in a delayed spread of a segregating mutation. Indeed, Orr and Betancourt (2001)

331   demonstrated that the bias against fixation of recessive alleles disappears when positive selection

332   acts on pre-existing variation in mutation-selection balance. We used simulations to test whether

333   different estimates of the timing of hybridization (i.e., the origin of the winter-brown haplotype)

334   and TMRCA of the winter-brown allele could be due to the masking of recessive alleles at low

335   frequency. Using SLiM 3.1 (Haller and Messer 2019), we simulated an equilibrium population

336   (N_e=257219 for OR population; Table 1) experiencing positive selection on a recessive allele

337   (s=0.026, which reflects our updated median estimate of s for winter-brown haplotype in OR;

338   Jones et al. 2018). At the beginning of the simulations, the recessive allele was introduced at a

339   rate of 0.01% or 0.1% per generation for 1 or 100 generations, which reflects various rates and

340   durations of hybridization. Under each hybridization scenario, we performed 100 simulations

341   and tracked the frequency of the recessive allele every generation, conditioning on fixation. We

342   saved tree sequences (Haller et al. 2019) and analyzed them using *msprime* (Kelleher et al. 2016)

343   to identify the TMCRA for fixed beneficial alleles and determine whether selection resulted in

344   fixation of a single copy (hard sweep) or multiple copies (soft sweep) of the beneficial allele.

345

346   **Results**

347   <u>Range-edge population history and mutational load</u>

348   We found support for a single relatively strong N contraction (i.e., a two-epoch model) occurring

349   ~24-100 kya in OR, WA, and BC hares (Table 1, Fig. S2). In contrast, the history of the MT

350   population was characterized by an instantaneous + exponential N change model, in which the

15

351 population experienced a sudden 17× expansion ~129 kya followed by a gradual reduction to

352 ~53% of N_{anc}. Despite population contractions, estimates of contemporary N_e across all

353 populations were relatively large (161654-257219; Table 1).

354   Using the same exome data set, we previously estimated the joint SFS for pairs of

355 snowshoe hare populations to infer histories of population split times, migration rates, and

356 effective population size in $\partial a \partial i$ (Jones et al. 2018). These pairwise models supported histories

357 of high symmetrical migration rates between populations and N contractions following

358 population splits, but generated significantly smaller estimates of contemporary N_e compared to

359 the new estimates that we report in Table 1. However, we made a scaling error while estimating

360 $\theta (= 4N_e\mu)$ under these previous models. This error affected our previously reported

361 demographic parameter estimates for snowshoe hares (Table S9 in Jones et al. 2018) and

362 associated selection coefficient parameter estimates (e.g., previous mean s_{WA}=0.024, s_{OR}=0.015;

363 updated mean s_{WA} =0.049, s_{OR}=0.027; Durrett and Schweinsberg 2005; Jones et al. 2018), but not

364 the main inference of introgression at *Agouti* underlying the genetic basis of polymorphic coat

365 color in snowshoe hares. After scaling parameter values to the correct value of θ and excluding

366 models beyond *a priori* divergence time parameter bounds (>500 thousand years), we found that

367 our maximum likelihood demographic model (reported here in Table S1) still includes high

368 migration rates between populations (~1-2.63 migrants per generation), but with appreciably

369 larger N_e estimates than we previously reported and that are comparable to our new estimates

370 (Table 1).

371   We found significantly elevated F_{IS} in the coastal BC population compared to the other

372 three PNW populations (*p*<0.01; Fig. 1B), which combined with our previous inference of

373 elevated LD in this population (Jones et al. 2018) could suggest recent inbreeding and population

16

374   size reduction. We further found a significantly higher proportion of homozygosity for

375   synonymous, nonsynonymous, and nonsense SNPs in BC relative to other populations (Fig. 1C),

376   which suggests elevated mutational load in BC under a recessive deleterious mutation model. BC

377   individuals also have a significantly higher proportion of strongly deleterious nonsynonymous

378   variants in (27.7%; $|s| \geq 10^{-3}$) relative to other populations (0.8-3.2%; Fig. 1D, Table S2). Because

379   we have the same sample size for MT and BC (n=14 individuals) this striking difference in the

380   DFE is likely not the result of the small BC sample size, which can lead to overestimation of the

381   proportion of strongly deleterious variation (Kim et al. 2017). Notably, if synonymous SNPs

382   used for demographic inference experience direct or linked selection (e.g., Akashi 1994;

383   Stoletzki and Eyre-Walker 2006; Resch et al. 2007; Pouyet et al. 2018), then our demographic

384   model could be misinferred (Ewing and Jensen 2016) in such a way that we will underestimate

385   the strength of purifying selection on non-synonymous SNPs. Regardless, assuming levels of

386   linked selection are similar across populations, the relative differences we observe in the DFE

387   are unlikely driven by weak or linked selection on synonymous variants.

388

389   The history of hybridization and introgression

390   From our complete mtDNA assemblies, we estimated a divergence time of 3.299 million

391   generations ago (95% HPD interval: 2.555-4.255 million generations ago; Fig. 2) between black-

392   tailed jackrabbit and non-introgressed snowshoe hares, which is consistent with previous

393   estimates of species' split times (Matthee et al. 2004; Melo-Ferreira et al. 2014; Jones et al.

394   2018). Within the non-introgressed snowshoe hare mtDNA clade, we found a relatively deep

395   split between the UT snowshoe hare (representing the 'Rockies' cluster identified by Cheng et al.

17

396   2014) and all other snowshoe hares (641 thousand generations ago, 95% HPD interval: 476-834

397   thousand generations ago; Fig. 2).

398   A significant portion of snowshoe hares from the PNW (100% of OR hares and 50% of

399   WA hares) formed a reciprocally monophyletic clade relative to black-tailed jackrabbits (100%

400   posterior node support; Fig. 2). As previously demonstrated through coalescent simulations

401   (Melo-Ferreira et al. 2014), this phylogenetic pattern cannot be plausibly explained by ILS and is

402   consistent with asymmetric introgression of black-tailed jackrabbit mtDNA into snowshoe hares.

403   As expected, mtDNA was not associated with winter coat color in the PNW polymorphic zone

404   (chi-squared P=1). However, if we assume that hybridization is rare then mtDNA may track the

405   same hybridization event that introduced winter-brown *Agouti* variation into PNW hares. The

406   estimated split time between black-tailed jackrabbit and introgressed PNW hare mtDNA

407   sequences was 516 thousand generations ago (95% HPD interval: 381-668 thousand generations

408   ago, Fig. 2). However, this split time does not account for segregating ancestral polymorphism

409   (Arbogast et al. 2002) or unsampled mtDNA variation within black-tailed jackrabbits. If we

410   assume extant variation in snowshoe hares represents a single mtDNA introgression event, then

411   the TMRCA of introgressed PNW snowshoe hare variation suggests a more recent date of

412   mtDNA introgression of ~228 thousand generations ago (95% HPD interval: 168-301 thousand

413   generations ago).

414   Our previous work revealed elevated signatures of genome-wide nuclear admixture

415   presumably coincident with introgression of seasonal camouflage variation (Jones et al. 2018).

416   Here we identified 1878 individual introgression tracts (median length = 28,940 bp),

417   encompassing ~1.99% of the genome (Fig. 3). Across various simulated hybridization scenarios,

418   the most strongly supported age of hybridization was 7-9 thousand generations ago with ranges

18

419   of 95% confidence intervals spanning 6-10.5 thousand generations ago (Fig. S4). Different rates

420   of admixture or admixture pulse lengths appeared to have little effect on the inferred

421   hybridization age or the overall fit to empirical data (Fig. S4). Furthermore, we observed poor

422   model fitting for very recent hybridization (< 5 thousand generations ago).

423

424   <u>Positive selection for winter-brown camouflage</u>

425   We identified the *Agouti* region as one of the longest (209,012 bp) and most highly supported

426   introgression tracts (mean introgression probability=0.99) in the WA winter-brown hare (Fig. 4).

427   To understand the history of positive selection on brown winter camouflage, we estimated the

428   TMRCA of the selected winter-brown *Agouti* haplotype in snowshoe hares using targeted

429   sequencing across the *Agouti* region (mean coverage per interval $34\times \pm 17\times$). Using a divergent

430   population, a local population, or both to represent the ancestral haplotype had little effect on

431   TMRCA estimates (Table S3), so here we present estimates using both populations. Under a low

432   or high estimate of the rabbit mutation rate, we inferred a TMRCA of approximately 1278

433   generations (95% CI: 1135-1441 generations) or 1226 generations (95% CI: 1054-1408

434   generations) for the winter-brown OR haplotype and approximately 1392 generations (95% CI:

435   1153-1607 generations) or 972 generations (95% CI: 766-1169 generations) for the WA

436   haplotype, respectively (Table S3). We observed no consistent allelic differences between the

437   fixed haplotypes in WA and OR (Fig. 4), consistent with a hard selective sweep.

438   Haplotype-based methods are known to underestimate the TMRCA and accounting for

439   this systematic error produces TMRCA estimates of approximately 2-4 thousand generations (for

440   a fully recessive allele, $\log_2(\text{estimate/true})\approx-1.5$; Kelley 2012) for the winter-brown haplotype in

441   OR and WA. If our estimates are accurate, then there appears to be a ~3-8 thousand generation

19

442   lag between the origin of the winter-brown haplotype in snowshoe hares (i.e., the inferred

443   hybridization date ~ 7-9 thousand generations ago) and the increase in frequency of the winter-

444   brown haplotype in the PNW from a single copy. Simulations show that such temporal lags are

445   expected for selection on recessive variation, however the duration of this lag (and the total

446   sojourn time) is negatively associated with the hybridization rate and fixation probability, as

447   expected (Table 2). For instance, under the lowest hybridization rate (0.01% for 1 generation) the

448   mean lag time was 2140 generations (95% CI: 101-8322 generation) with only a 0.8% fixation

449   probability and under the highest hybridization rate (0.1% for 100 generations) the mean lag time

450   was only 625 generations but with 100% fixation probability. Conditional on fixation, increased

451   hybridization rates also tended to be more often associated with soft rather than hard sweeps

452   (e.g., 38% hard sweeps for 0.1% hybridization rate for 100 generations versus 98% hard sweeps

453   for 0.01% hybridization rate for 1 generation). However, under intermediate hybridization

454   scenarios (0.1% for 1 generation or 0.01% for 100 generations), we observed relatively long

455   mean lag times (2514 and 1587 generations, respectively) associated with high probabilities of

456   fixation (12% and 79%, respectively), often through hard selective sweeps (81% and 96%; Table

457   2).

458

459   **Discussion**

460   Range-edge adaptation may enhance a species' evolutionary resilience to environmental change

461   (Hampe and Petit 2005; Hill et al. 2011), however rigorous population genetic evaluations of

462   predictions for range-edge demography and adaptation are limited (Bridle and Vines 2007). In

463   snowshoe hares, the evolution of brown winter coats in temperate climates along the PNW coast

464   represents the clearest example of local phenotypic adaptation in this wide-ranging species.

20

465   Given its direct link to reduced snow cover, the evolution of brown winter camouflage may

466   further foster persistence of snowshoe hares in the face of climate change (Mills et al. 2018).

467   Here we leveraged our understanding of the genetic basis of brown winter camouflage to

468   examine the history of range-edge adaptation, lending insights into the potential for rapid

469   adaptation following environmental change.

470

471   Population history and mutational load at the range edge

472   Populations along range margins are predicted to be small, limiting their ability to adapt to local

473   conditions (although see Moeller et al. 2011; Graignic et al. 2018). Although we cannot assess

474   relative differences in N_e across the entire hare range, we uncovered high N_e estimates across

475   PNW populations (161654-257219; Table 1), despite evidence for strong ancient population size

476   reductions. However, our N_e estimates derive from predictions of genetic drift (i.e., variance N_e)

477   over long evolutionary time scales and may be a weak reflection of current census sizes,

478   especially if local populations experience migration (Wang and Whitlock 2003) or have

479   undergone recent size changes that are undetectable with the SFS (Beichman et al. 2018). We

480   found evidence of significantly higher inbreeding coefficients and mutational load in coastal

481   (BC) populations relative to the inland and montane populations (Fig. 1), signatures that are

482   indicative of a recent population size reduction (Peischl et al. 2013, 2015; Bosshard et al. 2017;

483   Gilbert et al. 2018). Elevated F_{IS} and LD (Fig. S1 in Jones et al. 2018) could instead be related to

484   cryptic population substructure (i.e., the Wahlund effect; Waples 2015). However, we have

485   found no evidence for substructure or admixture in BC that could produce this effect (Jones et al.

486   in prep). Similar signatures of elevated mutational load (e.g., homozygosity for deleterious

487   alleles) have been found in other range-front populations, including the plant *Mercurialis annua*

21

488   (González-Martínez et al. 2017) and in human populations that migrated out of Africa (Henn et

489   al. 2016, although see Simons and Sella 2016). Thus, an intriguing potential explanation for

490   these patterns is that they reflect signatures of a founder event associated with a recent range

491   expansion. Moreover, given that we observe these signatures in the coastal winter-brown

492   population, it is possible that this expansion was enabled by the evolution of locally adaptive

493   brown winter camouflage. Winter-white hares experience heavy predation when mismatched

494   (Zimova et al. 2016) and are not known to occur in low-lying coastal regional west of the

495   Cascade Range (Nagorsen 1983; Mills et al. 2018), suggesting that coastal environments with

496   ephemeral snow cover were likely unoccupied prior to local camouflage adaptation.

497   Long-term persistence of populations under environmental change ultimately requires

498   adaptive evolution and the ability to colonize novel environments. If the colonization of coastal

499   PNW environments by snowshoe hares was enabled by the evolution of brown winter coats, our

500   results underscore that local adaptation to new environments can act as a negative feedback on

501   fitness through the accumulation of deleterious mutations (Pujol and Pannell 2008; Gilbert et al.

502   2017; González-Martínez et al. 2017; Stewart et al. 2017; Willi et al. 2018). Although the

503   consequences of mutational load for the persistence of PNW hare populations is unclear, high

504   recessive mutational load may compromise the adaptive potential of populations (Assaf et al.

505   2015; González-Martínez et al. 2017) and increase the probability of extinction in small

506   populations (Mills and Smouse 1994; Frankham 1998). In experiments of isolated *Tribolium*

507   populations, short-term fitness gains via adaptive evolution were entirely lost over longer time

508   periods as a consequence of increasing mutational load, although fitness could be readily

509   restored through admixture (Stewart et al. 2017). In snowshoe hares, the potential fitness costs

510   linked to mutational load may be mitigated by high gene flow between populations (Table S1) or

511   superseded by the enhanced species-level evolutionary resilience afforded by brown-winter

512   camouflage during periods of declining snow cover. Regardless, we suggest that any

513   conservation efforts to promote adaptation to climate change should weigh the potential for

514   enhanced long-term population persistence against the potential short-term fitness costs that may

515   arise through mutational load.

516

517   <u>Hybridization and the origin of the winter-brown allele</u>

518   Hybridization may play an important role shaping adaptation and expansion of range-edge

519   populations (Pfennig et al. 2016), but evidence for this mode of adaptation stems from only a

520   handful of examples (e.g., flies, Lewontin and Birch 1966; mosquitoes, Besansky et al. 2003;

521   sunflowers, Rieseberg et al. 2007). In snowshoe hares, range and niche expansion into mild

522   PNW coastal environments appears to have been enabled by adaptive introgression, although the

523   history of hybridization has remained unclear. We estimated that mtDNA introgression in PNW

524   snowshoe hares occurred ~228 thousand generations ago, which could be interpreted as a

525   conservative upper-bound for the timing of hybridization with black-tailed jackrabbits.

526   Meanwhile, the genome-wide distribution of introgression tract lengths, which should be less

527   sensitive to ILS and population structure within hares (Liu et al. 2014), suggest a much more

528   recent pulse of hybridization ~7-9 thousand generations ago (Fig. 3, Fig. S5). The different

529   genome-wide and mtDNA estimates may also reflect independent pulses of ancient

530   hybridization. Severe systematic overestimation of divergence dates may be common with

531   mtDNA genomes calibrated with a relatively divergent outgroup because of high mutation rates

532   and substitution saturation (Zheng et al. 2011). The divergence dates among major snowshoe

533   hare mtDNA lineages also appear much deeper than our best estimates derived from population

23

534   (nuclear) genomic data (~2-3 fold deeper, unpublished data), which suggests that our analyses

535   based on mtDNA likely overestimate the timing of introgression. We assumed a relatively simple

536   molecular clock model and more complicated models (e.g., relaxed clocks) might better account

537   for mutational processes observed in mtDNA genomes. However, it would seem that there would

538   be little insight to be gained by additional modeling here given the myriad of limitations

539   associated with extrapolating population history from a single stochastic realization of the

540   coalescent process (Hudson and Turelli 2003).

541   Several recent studies have also noted that introgression is positively correlated with local

542   recombination rate (Nachman and Payseur 2012; Janoušek et al. 2015; Schumer et al. 2018;

543   Edelman et al. 2019; Li et al. 2019; Martin et al. 2019), presumable due to the effects of linked

544   selection against deleterious mutations in hybrids. If this relationship generally holds, then it is

545   possible that our dating approach based on the distribution of introgression tract lengths is also

546   upwardly biased. However, contemporary range overlap between snowshoe hares and black-

547   tailed jackrabbits appears restricted to relatively sharp ecological transitions between sage-scrub

548   and montane forests in OR and CA (Fig. 2) and no records exist of putative hybrids, suggesting

549   that contemporary hybridization is likely exceedingly rare or absent and has not resulted in

550   discernable gene flow. Thus, the collective evidence suggests that historical hybridization

551   between snowshoe hares and black-tailed jackrabbits was not more recent than 5 thousand

552   generations ago. Notably, the timing of genome-wide admixture, assuming 1-2 generations per

553   year in hares (Marboutin and Peroux 1995), appears coincident with the retreat of the Cordilleran

554   ice sheet from low-lying coastal habitats in southern BC and northern WA at the end of the last

555   glacial maximum (~18 thousand years ago; Darvill et al. 2018) and thus the opening of suitable

556   habitat for winter-brown snowshoe hares. This period of rapid climatic change resulted in

24

557   individualistic range shifts for many North American mammal species (Graham 1986),

558   potentially leading to novel community assemblages and thus promoting hybridization events

559   (Swenson and Howard 2005), which could have created conditions favorable to adaptive

560   introgression.

561

562   <u>The spread of winter-brown camouflage and the tempo of local adaptation</u>

563   Although theory predicts adaptation in small range-edge populations may be slow and

564   mutation-limited, hybridization may alleviate the lack of beneficial variation along range

565   margins (Pfennig et al. 2016). Revealing how introgressed alleles adaptively spread through

566   populations is therefore a critical component of understanding the limitations of range-edge

567   adaptation. Here, we identified *Agouti* as one of the largest (>200 kb) and most strongly

568   supported introgression tracts genome-wide (Fig. 4), consistent with our previous study showing

569   exceptionally low genomic divergence in this region between black-tailed jackrabbits and

570   winter-brown snowshoe hares (Jones et al. 2018). Assuming our genome-wide estimates of

571   hybridization age reflect the origination of the *Agouti* allele through introgression (~9 thousand

572   generations ago), our findings suggest a ~3-8 thousand generation delay until the selective sweep

573   of the winter-brown haplotype in the PNW.

574   One potential biological explanation for this temporal lag is that winter-brown

575   camouflage was not immediately beneficial in snowshoe hares. Rather, the winter-brown variant

576   may have initially segregated as a neutral or deleterious allele for a period of time until an

577   environmental shift allowed positive selection to act quickly on standing variation (e.g.,

578   Colosimo et al. 2005). However, our simulations suggest that beneficial recessive alleles

579   segregating at frequencies as high as ~10% (equivalent to simulations of 0.1% hybridization rate

25

580   for 100 generations) take on average ~5612 generations (95% CI: 4319-6757 generations) to

581   reach fixation (Table 2). Thus, under an environmental shift scenario, the starting frequency of

582   the winter-brown variant would likely have to be quite large (>10%) in order for selection to

583   quickly drive it to fixation. Although allelic fixation under this model would be virtually

584   guaranteed (Table 2), we suspect that such a high level of hybridization between black-tailed

585   jackrabbits and snowshoe hares is unlikely given their ecological distinctiveness and our lower

586   estimate of the genome-wide proportion of introgression (~1.99%). Furthermore, the high

587   starting allele frequency needed to result in rapid fixation is at odds with the evidence that

588   selection fixed a single haplotype, as higher hybridization rates tended to result in softer sweeps

589   (Table 2).

590   An alternative explanation for the delayed rise in frequency of the winter-brown allele

591   invokes the limits of positive selection on recessive variation, which is predicted to result in an

592   extended period of drift while at low frequency until homozygous recessive genotypes become

593   more common. Consistent with this, we find significant temporal lags between the timing of

594   hybridization and the TMRCA of fixed beneficial recessive alleles under low and moderate rates

595   of hybridization. Although fixation under our lowest simulated rate of hybridization was highly

596   unlikely (~0.8%; Table 2), the two intermediate scenarios still resulted in relatively high fixation

597   probabilities (12-78%) and tended to produce hard sweeps (81-96%), consistent with observed

598   patterns of genetic variation at the winter-brown *Agouti* haplotype. These results demonstrate

599   that one does not need to invoke changing selective coefficients to explain the apparent lag

600   between the origin and the TMRCA of the winter-brown allele. Rather, our data are consistent

601   with the winter-brown variant being immediately beneficial, although predominately hidden to

602   selection, after introduced through hybridization at moderate frequency (~0.1-1%). Indeed, this

26

603   mutation-limited scenario is consistent with other known instances of colonization of novel

604   environments through the evolution of locally adaptive camouflage in Nebraska deer mice and

605   White Sands lizards (Laurent et al. 2016; Pfeifer et al. 2018; Harris et al. 2019).

606   Rates of adaptation at range edges are potentially an important component of species'

607   responses to climate change (Hampe and Petit 2005). Our study highlights the key role that

608   hybridization can play in seeding adaptive variation and facilitating range expansion during

609   periods of environmental change. In some cases, introgression appears to facilitate rapid

610   adaptation to environmental change (Norris et al. 2015; Oziolor et al. 2019). However,

611   introgression may not always be an efficient solution for rapid adaptation, as here we

612   demonstrate that the rate of adaptation to novel mild winter environments in snowshoe hares

613   appears to have been limited by the dominance coefficient of the winter-brown allele.

614   Collectively, our findings demonstrate key factors that promote and limit adaptation to changing

615   environments and, in particular, highlight the importance of characterizing genetic dominance of

616   beneficial variants for understanding rates of adaptation and range expansion under climate

617   change.

618

Acknowledgements

632

633

Figure 1. (A) Snowshoe hare range map colored by the probability of winter-white camouflage

(white=1, brown=0). The Pacific Northwest region is magnified and shows sampling localities

29

636   and coat color phenotypes for BC (purple), MT (red), OR (green), and WA (blue) populations

637   used to generate whole exome data. (**B**) Box-and-whisker plots representing distributions of

638   individual inbreeding coefficients (F_{IS}) within each population. (**C**) The proportion of

639   homozygosity across PNW populations for SNPs classified as synonymous, nonsynonymous

640   (missense), or nonsense. Different letters denote significant differences between populations

641   ($p<0.01$). (**D**) The inferred distribution of fitness effects for each population shown as the

642   proportion of mutations with given selection coefficients.

643

644
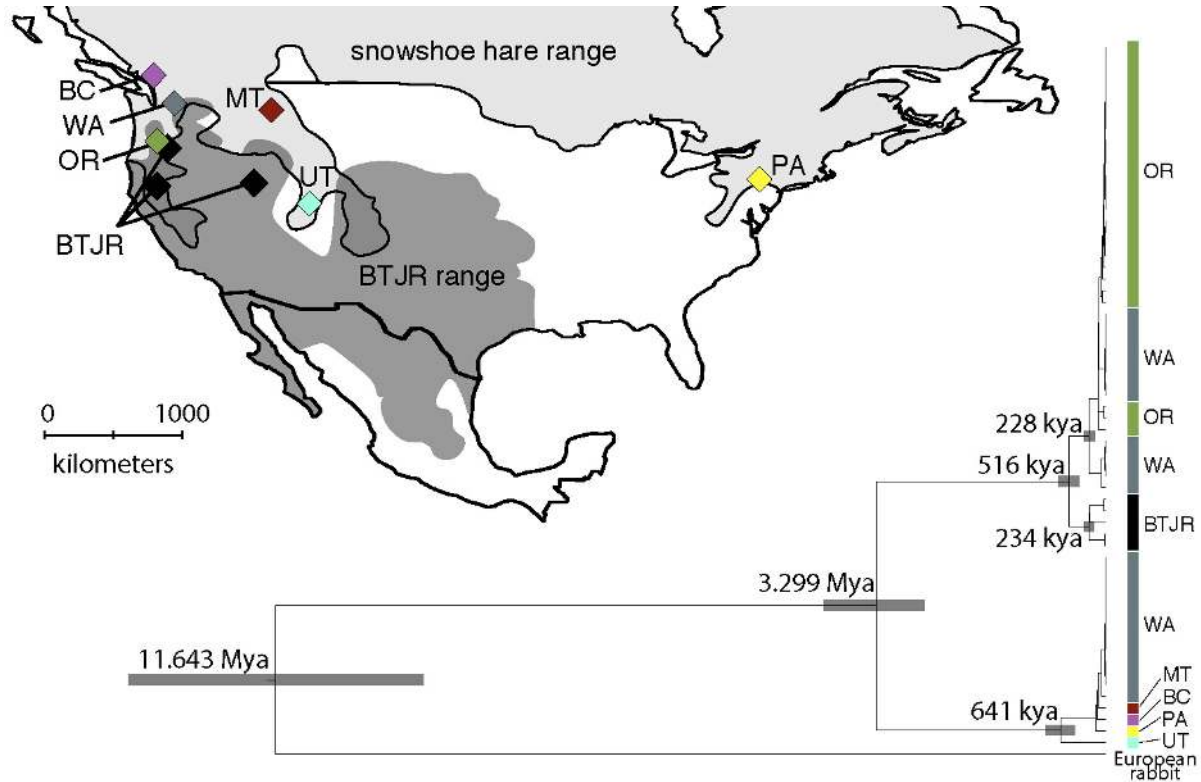
Figure 2. Snowshoe hare and black-tailed jackrabbit (BTJR) ranges with sampling localities for whole genome sequencing. The phylogenetic tree is a maximum clade credibility tree based on whole mitochondrial genome assemblies of snowshoe hares and black-tailed jackrabbits (European rabbit as outgroup) with median estimated split times for crucial nodes. Sample locality names and colors correspond to those on the map. Gray rectangles show the 95% highest posterior density (HPD) for each node age estimate.
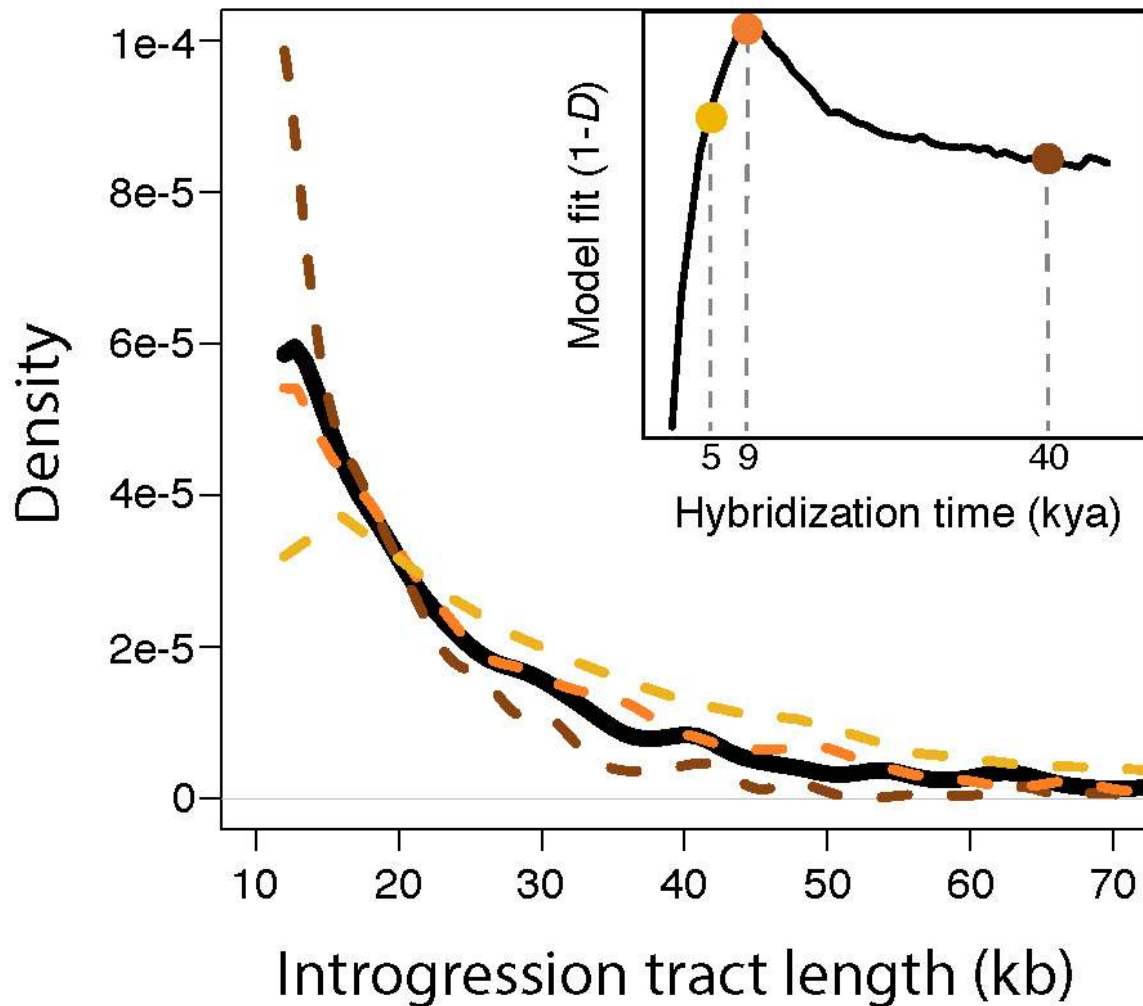
651

652 **Figure 3.** Empirical and simulated distributions of introgression tract lengths. The black line

653 shows the empirical distribution of genome-wide introgression tract lengths in snowshoe hares.

654 Colored dashed lines show simulated tract length distributions at three time points following a

655 100 generation pulse of hybridization at 0.1% frequency (yellow= 5 kya, orange=9 kya,

656 brown=40 kya). The inset figure shows the overall fit of simulated introgression tract lengths to

657 the empirical distribution through time, with hybridization occurring 9 kya as the model with the

658 strongest fit (95% confidence intervals: 8-10.5 kya).

659
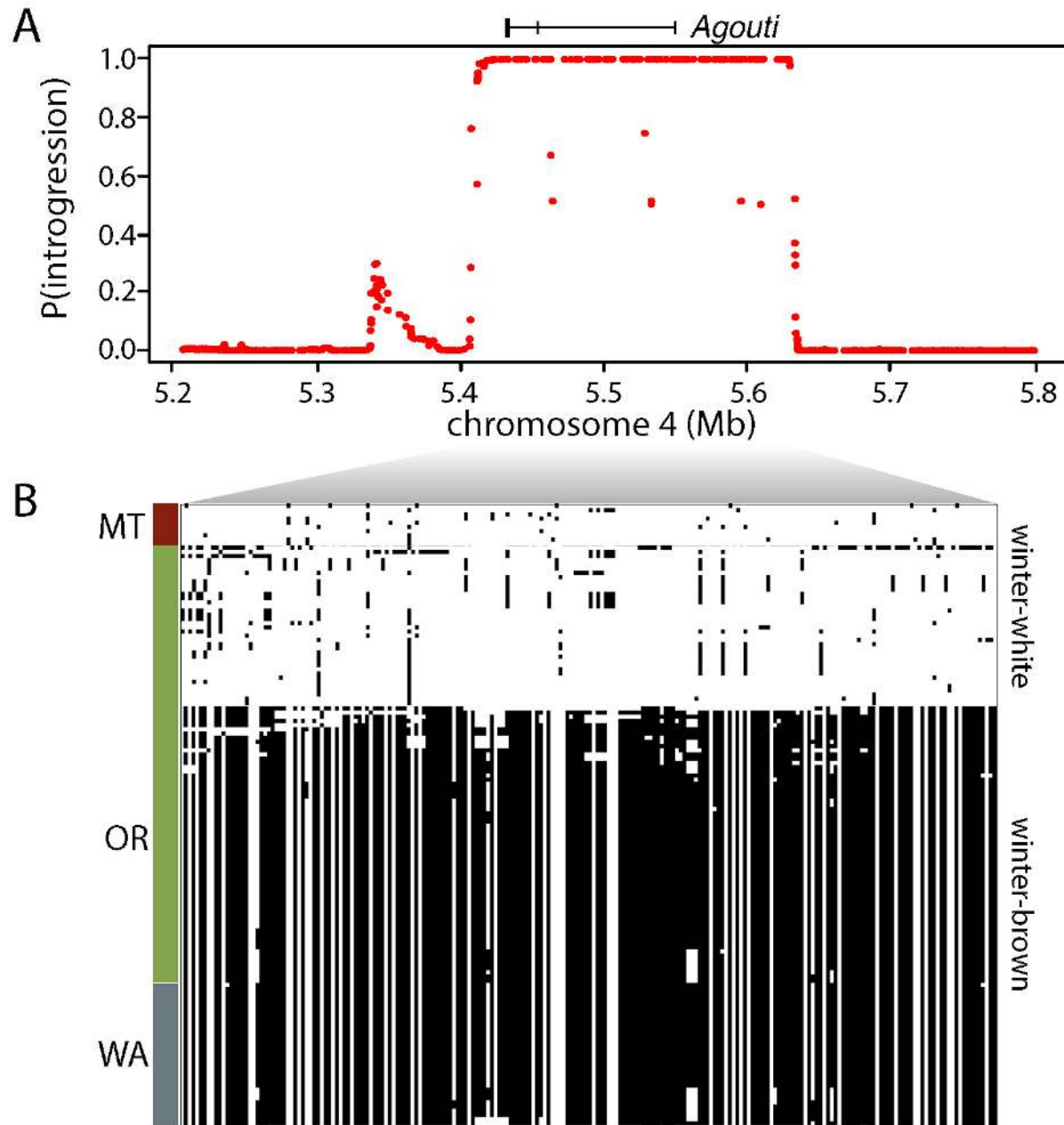
Figure 4. (**A**) Phylonet-HMM classification of the probability of introgression for each variable

position across the *Agouti* locus. (**B**) Haplotype structure across the inferred introgressed *Agouti*

interval (chr4:5424111-5633123) for winter-white and winter-brown PNW snowshoe hares.

663

664

665 **Table 1. Maximum likelihood demographic model parameter estimates**.

Population	Model	N_{anc}	N_B	N_F	t (generations)
MT	Inst. change + exp. growth	459809 (450035-469582)	8121810 (5984297-10344665)	245430 (197252-295473)	129400 (98087-161953)
BC	Two-epoch	669265 (662769-675760)	210484 (184353-237086)	-	97853 (70702-125517)
WA	Two-epoch	509979 (503464-516493)	161654 (125444-198747)	-	24357 (20061-28755)
OR	Two-epoch	494903 (482587-507220)	257219 (191394-326076)	-	52540 (44017-61431)

666 Values in parentheses are the 95% confidence intervals. N_{anc} = population size of common

667 ancestor; N_B = population size following instantaneous change at time t. N_F is the population size

668 following an exponential change beginning immediately after time t.

34

669   **Table 2. Results from simulations of positive selection on recessive variation**.

	1 generation pulse		100 generation pulse	
	0.01%	**0.1%**	**0.01%**	**0.1%**
P(fixation)	0.0082 (0.0068-0.010)	0.12 (0.098-0.13)	0.79 (0.71-0.85)	1.0 (0.96-1.0)
P(hard sweep)	0.98 (0.93-0.99)	0.81 (0.72-0.87)	0.96 (0.90-0.98)	0.38 (0.29-0.48)
T(sojourn)	8911 (5179-16208)	9448 (5626-15746)	6472 (5088-15339)	5612 (4319-6757)
T(lag)	2140 (101-8322)	2514 (97-7740)	1587 (87-7253)	624 (91-1899)

670   The beneficial variant was introduced through hybridization during a 1 or 100 generation pulse at

671   a rate of 0.01% or 0.1%. Data are shown for the probability of fixation (P(fixation)), and,

672   conditional on fixation, the probability of a hard selective sweep(P(hard sweep)), the mean

673   sojourn time (T(sojourn)), and the mean lag time between a fixed mutation's origin and TMRCA

674   (T(lag)). In parentheses are 95% confidence intervals.

35

References

Ackerly, D. D. 2003. Community assembly, niche conservatism, and adaptive evolution in changing environments. International Journal of Plant Sciences 164:S165–S184.

Akashi, H. 1994. Synonymous codon usage in *Drosophila melanogaster*: natural selection and translational accuracy. Genetics 136:927–935.

Antonovics, J. 1976. The nature of limits to natural selection. Annals of the Missouri Botanical Garden 63:224–247.

Arbogast, B. S., S. V. Edwards, J. Wakeley, P. Beerli, and J. B. Slowinski. 2002. Estimating divergence times from molecular data on phylogenetic and population genetic timescales. Annual Review of Ecology and Systematics 33:707–740.

Assaf, Z. J., D. A. Petrov, and J. R. Blundell. 2015. Obstruction of adaptation in diploids by recessive, strongly deleterious alleles. Proceedings of the National Academy of Sciences of the United States of America 112:E2658-66.

Baker, H. G. 1948. Stages in invasion and replacement demonstrated by species of *Melandrium*. The Journal of Ecology 36:96–119.

Barton, N. 2001. Adaptation at the edge of a species' range. Pages 365–392 *in* J. Silvertown and J. Antonovics, eds. Integrating ecology and evolution in a spatial context. Blackwell Science.

Behrman, K. D., and M. Kirkpatrick. 2011. Species range expansion by beneficial mutations. Journal of Evolutionary Biology 24:665–675.

Beichman, A. C., E. Huerta-Sanchez, and K. E. Lohmueller. 2018. Using genomic data to infer historic population dynamics of nonmodel organisms. Annual Review of Ecology, Evolution, and Systematics 49:433–56.

Besansky, N. J., J. Krzywinski, T. Lehmann, F. Simard, M. Kern, O. Mukabayire, D. Fontenille, et al. 2003. Semipermeable species boundaries between *Anopheles gambiae* and *Anopheles arabiensis*: evidence from multilocus DNA sequence variation. Proceedings of the National Academy of Sciences of the United States of America 100:10818–23.

Bolger, A. M., M. Lohse, and B. Usadel. 2014. Trimmomatic: a flexible trimmer for Illumina sequence data. Bioinformatics 30:2114–2120.

Bontrager, M., and A. L. Angert. 2019. Gene flow improves fitness at a range edge under climate change. Evolution Letters 3:55–68.

Bosshard, L., I. Dupanloup, O. Tenaillon, R. Bruggmann, M. Ackermann, S. Peischl, and L. Excoffier. 2017. Accumulation of deleterious mutations during bacterial range expansions. Genetics 207:669–684.

Bouckaert, R., J. Heled, D. Kühnert, T. Vaughan, C.-H. Wu, D. Xie, M. A. Suchard, et al. 2014. BEAST 2: a software platform for bayesian evolutionary analysis. PLoS Computational Biology 10:e1003537.

Bridle, J. R., and T. H. Vines. 2007. Limits to evolution at range margins: when and why does adaptation fail? Trends in Ecology & Evolution 22:140–147.

Browning, S. R., and B. L. Browning. 2007. Rapid and accurate haplotype phasing and missing-data inference for whole-genome association studies by use of localized haplotype clustering. The American Journal of Human Genetics 81:1084–1097.

Burke, J. M., and M. L. Arnold. 2001. Genetics and the fitness of hybrids. Annual Review of Genetics 35:31–52.

Carneiro, M., S. Afonso, A. Geraldes, H. Garreau, G. Bolet, S. Boucher, A. Tircazes, et al. 2011.

721   The genetic structure of domestic rabbits. Molecular Biology and Evolution 28:1801–
722   1816.
723 Carneiro, M., F. W. Albert, J. Melo-Ferreira, N. Galtier, P. Gayral, J. A. Blanco-Aguiar, R.
724   Villafuerte, et al. 2012. Evidence for widespread positive and purifying selection across
725   the European rabbit (*Oryctolagus cuniculus*) genome. Molecular Biology and Evolution
726   29:1837–1849.
727 Carneiro, M., C.-J. Rubin, F. Di Palma, F. W. Albert, J. Alföldi, A. Martinez Barrio, G. Pielberg,
728   et al. 2014. Rabbit genome analysis reveals a polygenic basis for phenotypic change
729   during domestication. Science 345:1074–1079.
730 Cheng, E., K. E. Hodges, J. Melo-Ferreira, P. C. Alves, and L. S. Mills. 2014. Conservation
731   implications of the evolutionary history and genetic diversity hotspots of the snowshoe
732   hare. Molecular Ecology 23:2929–2942.
733 Cingolani, P., A. Platts, L. L. Wang, M. Coon, T. Nguyen, L. Wang, S. J. Land, et al. 2012. A
734   program for annotating and predicting the effects of single nucleotide polymorphisms,
735   SnpEff: SNPs in the genome of *Drosophila melanogaster* strain w1118; iso-2; iso-3. Fly
736   6:80–92.
737 Coffman, A. J., P. H. Hsieh, S. Gravel, and R. N. Gutenkunst. 2016. Computationally efficient
738   composite likelihood statistics for demographic inference. Molecular Biology and
739   Evolution 33:591–593.
740 Colosimo, P. F., K. E. Hosemann, S. Balabhadra, G. Villarreal, M. Dickson, J. Grimwood, J.
741   Schmutz, et al. 2005. Widespread parallel evolution in sticklebacks by repeated fixation
742   of *Ectodysplasin* alleles. Science 307:1928–1933.
743 Corbett-Detig, R., and M. Jones. 2016. SELAM: simulation of epistasis and local adaptation
744   during admixture with mate choice. Bioinformatics 32:3035–3037.
745 Danecek, P., A. Auton, G. Abecasis, C. A. Albers, E. Banks, M. A. DePristo, R. E. Handsaker, et
746   al. 2011. The variant call format and VCFtools. Bioinformatics 27:2156–2158.
747 Darvill, C. M., B. Menounos, B. M. Goehring, O. B. Lian, and M. W. Caffee. 2018. Retreat of
748   the western Cordilleran Ice Sheet margin during the last deglaciation. Geophysical
749   Research Letters 45:9710–9720.
750 Dierckxsens, N., P. Mardulyn, and G. Smits. 2017. NOVOPlasty: de novo assembly of organelle
751   genomes from whole genome data. Nucleic Acids Research 45:e18.
752 Durrett, R., and J. Schweinsberg. 2005. A coalescent model for the effect of advantageous
753   mutations on the genealogy of a population. Stochastic Processes and their Applications
754   115:1628–1657.
755 Edelman, N. B., P. B. Frandsen, M. Miyagi, B. J. Clavijo, J. Davey, R. Dikow, G. Garcia-
756   Accinelli, et al. 2019. Genomic architecture and introgression shape a butterfly radiation.
757   Science 366:594–599.
758 Ewing, G. B., and J. D. Jensen. 2016. The consequences of not accounting for background
759   selection in demographic inference. Molecular Ecology 25:135–141.
760 Forsman, A. 2016. Is colour polymorphism advantageous to populations and species? Molecular
761   Ecology 25:2693–2698.
762 Frankham, R. 1998. Inbreeding and extinction: island populations. Conservation Biology
763   12:665–675.
764 Garcia-Ramos, G., and M. Kirkpatrick. 1997. Genetic models of adaptation and gene flow in
765   peripheral populations. Evolution 51:21–28.
766 Gigliotti, L. C., D. R. Diefenbach, and M. J. Sheriff. 2017. Geographic variation in winter

767   adaptations of snowshoe hares (*Lepus americanus*). Canadian Journal of Zoology
768   95:539–545.
769   Gilbert, K. J., S. Peischl, and L. Excoffier. 2018. Mutation load dynamics during
770   environmentally-driven range shifts. PLOS Genetics 14:e1007450.
771   Gilbert, K. J., N. P. Sharp, A. L. Angert, G. L. Conte, J. A. Draghi, F. Guillaume, A. L.
772   Hargreaves, et al. 2017. Local adaptation interacts with expansion load during range
773   expansion: maladaptation reduces expansion load. The American Naturalist 189:368–
774   380.
775   Gilbert, K., and M. C. Whitlock. 2016. The genetics of adaptation to discrete heterogeneous
776   environments: frequent mutation or large-effect alleles can allow range expansion.
777   Journal of Evolutionary Biology 30:591–602.
778   González-Martínez, S. C., K. Ridout, and J. R. Pannell. 2017. Range expansion compromises
779   adaptive evolution in an outcrossing plant. Current Biology 27:2544–2551.
780   Graham, R. W. 1986. Response of mammalian communities to environmental changes during the
781   late Quaternary. Pages 300–313 *in* D. J. and C. T. J., eds. Community Ecology. Harper &
782   Row, New York.
783   Graignic, N., F. Tremblay, and Y. Bergeron. 2018. Influence of northern limit range on genetic
784   diversity and structure in a widespread North American tree, sugar maple (*Acer
785   saccharum* Marshall). Ecology and Evolution 8:2766–2780.
786   Griffin, P. C., and L. S. Mills. 2009. Sinks without borders: Snowshoe hare dynamics in a
787   complex landscape. Oikos 118:1487–1498.
788   Gutenkunst, R. N., R. D. Hernandez, S. H. Williamson, and C. D. Bustamante. 2009. Inferring
789   the joint demographic history of multiple populations from multidimensional SNP
790   frequency data. PLoS Genetics 5:e1000695.
791   Haldane, J. B. S. 1924. A mathematical theory of natural and artificial selection Part I.
792   Transactions of the Cambridge Philosophical Society 23:19–41.
793   ———. 1930. A mathematical theory of natural and artificial selection (Part VI, Isolation).
794   Mathematical Proceedings of the Cambridge Philosophical Society 26:220–230.
795   Haller, B. C., J. Galloway, J. Kelleher, P. W. Messer, and P. L. Ralph. 2019. Tree-sequence
796   recording in SLiM opens new horizons for forward-time simulations of whole genomes.
797   Molecular Ecology Resources 19:552–566.
798   Haller, B. C., and P. W. Messer. 2019. SLiM 3: Forward genetic simulations beyond the Wright-
799   Fisher model. Molecular Biology and Evolution 36:632–637.
800   Hampe, A., and R. J. Petit. 2005. Conserving biodiversity under climate change: the rear edge
801   matters. Ecology Letters 8:461–467.
802   Harris, R. B., K. Irwin, M. R. Jones, S. Laurent, R. D. H. Barrett, R. D. H. Nachman, J. M. Good,
803   et al. 2019. The population genetics of crypsis in vertebrates: recent insights from mice,
804   hares, and lizards. Heredity doi:10.1038/s41437-019-0257-4.
805   Hedrick, P. W. 2013. Adaptive introgression in animals: examples and comparison to new
806   mutation and standing variation as sources of adaptive variation. Molecular Ecology
807   22:4606–4618.
808   Henn, B. M., L. R. Botigué, S. Peischl, I. Dupanloup, M. Lipatov, B. K. Maples, A. R. Martin, et
809   al. 2016. Distance from sub-Saharan Africa predicts mutational load in diverse human
810   genomes. Proceedings of the National Academy of Sciences of the United States of
811   America 113:E440-9.
812   Hill, J. K., H. M. Griffiths, and C. D. Thomas. 2011. Climate change and evolutionary

813   adaptations at species' range margins. Annual Review of Entomology 56:143–159.

814 Holt, R. D., and R. Gomulkiewicz. 1997. How does immigration influence local adaptation? A
815   reexamination of a familiar paradigm. The American Naturalist 149:563–572.

816 Hudson, R. R., and M. Turelli. 2003. Stochasticity overrules the "three-times rule": genetic drift,
817   genetic draft, and coalescence times for nuclear loci versus mitochondrial DNA.
818   Evolution 57:182–190.

819 Huerta-Sánchez, E., X. Jin, Asan, Z. Bianba, B. M. Peter, N. Vinckenbosch, Y. Liang, et al.
820   2014. Altitude adaptation in Tibetans caused by introgression of Denisovan-like DNA.
821   Nature 512:194–197.

822 Janoušek, V., P. Munclinger, L. Wang, K. C. Teeter, and P. K. Tucker. 2015. Functional
823   organization of the genome may shape the species boundary in the house mouse.
824   Molecular Biology and Evolution 32:1208–1220.

825 Jones, M. R., L. S. Mills, P. C. Alves, C. M. Callahan, J. M. Alves, D. J. R. Lafferty, F. M.
826   Jiggins, et al. 2018. Adaptive introgression underlies polymorphic seasonal camouflage
827   in snowshoe hares. Science 360:1355–1358.

828 Kawecki, T. J. 2008. Adaptation to marginal habitats. Annual Review of Ecology, Evolution, and
829   Systematics 39:321–342.

830 Keightley, P. D., and A. Eyre-Walker. 2010. What can we learn about the distribution of fitness
831   effects of new mutations from DNA sequence data? Philosophical Transactions of the
832   Royal Society B: Biological Sciences 365:1187–93.

833 Kelleher, J., A. M. Etheridge, and G. McVean. 2016. Efficient coalescent simulation and
834   genealogical analysis for large sample sizes. PLOS Computational Biology 12:e1004842.

835 Kelley, J. L. 2012. Systematic underestimation of the age of selected alleles. Frontiers in
836   Genetics 3:165.

837 Kim, B. Y., C. D. Huber, and K. E. Lohmueller. 2017. Inference of the distribution of selection
838   coefficients for new nonsynonymous mutations using large samples. Genetics 206:345–
839   361.

840 Kirkpatrick, M., and N. H. Barton. 1997. Evolution of a species' range. The American Naturalist
841   150:1–23.

842 Lamichhaney, S., J. Berglund, M. S. Almén, K. Maqbool, M. Grabherr, A. Martinez-Barrio, M.
843   Promerová, et al. 2015. Evolution of Darwin's finches and their beaks revealed by
844   genome sequencing. Nature 518:371–375.

845 Larkin, M. A., G. Blackshields, N. P. Brown, R. Chenna, P. A. McGettigan, H. McWilliam, F.
846   Valentin, et al. 2007. Clustal W and Clustal X version 2.0. Bioinformatics 23:2947–2948.

847 Laurent, S., S. P. Pfeifer, M. L. Settles, S. S. Hunter, K. M. Hardwick, L. Ormond, V. C. Sousa,
848   et al. 2016. The population genomics of rapid adaptation: disentangling signatures of
849   selection and demography in white sands lizards. Molecular Ecology 25:306–323.

850 Lewontin, R. C., and L. C. Birch. 1966. Hybridization as a source of variation for adaptation to
851   new environments. Evolution 20:315–336.

852 Li, G., H. V Figueiró, E. Eizirik, and W. J. Murphy. 2019. Recombination-aware phylogenomics
853   reveals the structured genomic landscape of hybridizing cat species. Molecular Biology
854   and Evolution 36:2111–2126.

855 Li, H. 2013. Aligning sequence reads, clone sequences and assembly contigs with BWA-MEM.
856   arXiv 1303.3997.

857 Liu, K. J., J. Dai, K. Truong, Y. Song, M. H. Kohn, and L. Nakhleh. 2014. An HMM-based
858   comparative genomic framework for detecting introgression in eukaryotes. PLoS

859   Computational Biology 10:e1003649.

860   Loh, P.-R., M. Lipson, N. Patterson, P. Moorjani, J. K. Pickrell, D. Reich, and B. Berger. 2013.
861   Inferring admixture histories of human populations using linkage disequilibrium.
862   Genetics 193:1233–1254.

863   Lynch, M., J. Conery, and R. Burger. 1995. Mutation accumulation and the extinction of small
864   populations. The American Naturalist 146:489–518.

865   Magoč, T., and S. L. Salzberg. 2011. FLASH: fast length adjustment of short reads to improve
866   genome assemblies. Bioinformatics 27:2957–2963.

867   Marboutin, E., and R. Peroux. 1995. Survival pattern of European hare in a decreasing
868   population. The Journal of Applied Ecology 32:809–816.

869   Marnetto, D., and E. Huerta-Sánchez. 2017. Haplostrips: revealing population structure through
870   haplotype visualization. Methods in Ecology and Evolution 8:1389–1392.

871   Martin, S. H., J. Davey, C. Salazar, and C. Jiggins. 2019. Recombination rate variation shapes
872   barriers to introgression across butterfly genomes. PLoS Biology 17:e2006288.

873   Massey, F. J. 1951. The Kolmogorov-Smirnov test for goodness of fit. Journal of the American
874   Statistical Association 46:68–78.

875   Matthee, C. A., B. J. Van Vuuren, D. Bell, and T. J. Robinson. 2004. A molecular supermatrix of
876   the rabbits and hares (Leporidae) allows for the identification of five intercontinental
877   exchanges during the Miocene. Systematic Biology 53:433–447.

878   McKenna, A., M. Hanna, E. Banks, A. Sivachenko, K. Cibulskis, A. Kernytsky, K. Garimella, et
879   al. 2010. The Genome Analysis Toolkit: A MapReduce framework for analyzing next-
880   generation DNA sequencing data. Genome Research 20:1297–1303.

881   Melo-Ferreira, J., F. A. Seixas, E. Cheng, L. S. Mills, and P. C. Alves. 2014. The hidden history
882   of the snowshoe hare, *Lepus americanus*: extensive mitochondrial DNA introgression
883   inferred from multilocus genetic variation. Molecular Ecology 23:4617–4630.

884   Meyer, M., and M. Kircher. 2010. Illumina sequencing library preparation for highly multiplexed
885   target capture and sequencing. Cold Spring Harbor Protocols 5:pdb.prot5448.

886   Miao, B., Z. Wang, and Y. Li. 2016. Genomic analysis reveals hypoxia adaptation in the Tibetan
887   Mastiff by introgression of the Grey Wolf from the Tibetan Plateau. Molecular Biology
888   and Evolution 34:734–743.

889   Mills, L. S., E. V Bragina, A. V Kumar, M. Zimova, D. J. R. Lafferty, J. Feltner, B. M. Davis, et
890   al. 2018. Winter color polymorphisms identify global hot spots for evolutionary rescue
891   from climate change. Science 359:1033–1036.

892   Mills, L. S., and P. E. Smouse. 1994. Demographic consequences of inbreeding in remnant
893   populations. The American Naturalist 144:412–431.

894   Mills, L. S., M. Zimova, J. Oyler, S. Running, J. T. Abatzoglou, and P. M. Lukacs. 2013.
895   Camouflage mismatch in seasonal coat color due to decreased snow duration.
896   Proceedings of the National Academy of Sciences of the United States of America
897   110:7360–7365.

898   Moeller, D. A., M. A. Geber, and P. Tiffin. 2011. Population genetics and the evolution of
899   geographic range limits in an annual plant. The American Naturalist 178:S44-61.

900   Nachman, M. W., and B. A. Payseur. 2012. Recombination rate variation and speciation:
901   theoretical predictions and empirical results from rabbits and mice. Philosophical
902   Transactions of the Royal Society B: Biological Sciences 367:409–421.

903   Nagorsen, D. W. 1983. Winter pelage colour in snowshoe hares (*Lepus americanus*) from the
904   Pacific Northwest. Canadian Journal of Zoology 61:2313–2318.

905 Nelson, T. C., M. R. Jones, J. P. Velotta, A. S. Dhawanjewar, and R. M. Schweizer. 2019.
906   UNVEILing connections between genotype, phenotype, and fitness in natural
907   populations. Molecular Ecology 28:1866–1876.
908 Norris, L. C., B. J. Main, Y. Lee, T. C. Collier, A. Fofana, A. J. Cornel, and G. C. Lanzaro. 2015.
909   Adaptive introgression in an African malaria mosquito coincident with the increased
910   usage of insecticide-treated bed nets. Proceedings of the National Academy of Sciences
911   of the United States of America 112:815–20.
912 Orr, H. A., and A. J. Betancourt. 2001. Haldane's sieve and adaptation from the standing genetic
913   variation. Genetics 157:875–884.
914 Oziolor, E. M., N. M. Reid, S. Yair, K. M. Lee, S. Guberman VerPloeg, P. C. Bruns, J. R. Shaw,
915   et al. 2019. Adaptive introgression enables evolutionary rescue from extreme
916   environmental pollution. Science 364:455–457.
917 Pardo-Diaz, C., C. Salazar, S. W. Baxter, C. Merot, W. Figueiredo-Ready, M. Joron, W. O.
918   McMillan, et al. 2012. Adaptive introgression across species boundaries in *Heliconius*
919   butterflies. PLoS Genetics 8:e1002752.
920 Peischl, S., I. Dupanloup, M. Kirkpatrick, and L. Excoffier. 2013. On the accumulation of
921   deleterious mutations during range expansions. Molecular Ecology 22:5972–5982.
922 Peischl, S., M. Kirkpatrick, and L. Excoffier. 2015. Expansion load and the evolutionary
923   dynamics of a species range. The American Naturalist 185:E81–E93.
924 Pfeifer, S. P., S. Laurent, V. C. Sousa, C. R. Linnen, M. Foll, L. Excoffier, H. E. Hoekstra, et al.
925   2018. The evolutionary history of Nebraska deer mice: local adaptation in the face of
926   strong gene flow. Molecular Biology and Evolution 35:792–806.
927 Pfennig, K. S., A. L. Kelly, and A. A. Pierce. 2016. Hybridization as a facilitator of species range
928   expansion. Proceedings of the Royal Society B: Biological Sciences 283:20161329.
929 Polechová, J. 2018. Is the sky the limit? On the expansion threshold of a species' range. PLoS
930   Biology 16:e2005372.
931 Pouyet, F., S. Aeschbacher, A. Thiéry, and L. Excoffier. 2018. Background selection and biased
932   gene conversion affect more than 95% of the human genome and bias demographic
933   inferences. eLife 7:e36317.
934 Pujol, B., and J. R. Pannell. 2008. Reduced responses to selection after species range expansion.
935   Science 321:96.
936 R Core Team. 2018. R: A language and environment for statistical computing. R Foundation for
937   Statistical Computing, Vienna, Austria.
938 Resch, A. M., L. Carmel, L. Mariño-Ramírez, A. Y. Ogurtsov, S. A. Shabalina, I. B. Rogozin,
939   and E. V. Koonin. 2007. Widespread positive selection in synonymous sites of
940   mammalian genes. Molecular Biology and Evolution 24:1821–1831.
941 Rieseberg, L. H., S.-C. Kim, R. A. Randell, K. D. Whitney, B. L. Gross, C. Lexer, and K. Clay.
942   2007. Hybridization and the colonization of novel habitats by annual sunflowers.
943   Genetica 129:149–165.
944 Robinson, J. D., A. J. Coffman, M. J. Hickerson, and R. N. Gutenkunst. 2014. Sampling
945   strategies for frequency spectrum-based population genomic inference. BMC
946   Evolutionary Biology 14:254.
947 Rohland, N., and D. Reich. 2012. Cost-effective, high-throughput DNA sequencing libraries for
948   multiplexed target capture. Genome Research 22:939–946.
949 Schumer, M., R. Cui, D. L. Powell, G. G. Rosenthal, and P. Andolfatto. 2016. Ancient
950   hybridization and genomic stabilization in a swordtail fish. Molecular Ecology 25:2661–

41

951   2679.
952 Schumer, M., C. Xu, D. L. Powell, A. Durvasula, L. Skov, C. Holland, J. C. Blazier, et al. 2018.
953   Natural selection interacts with recombination to shape the evolution of hybrid genomes.
954   Science 360:656–660.
955 Sgrò, C. M., A. J. Lowe, and A. A. Hoffmann. 2011. Building evolutionary resilience for
956   conserving biodiversity under climate change. Evolutionary Applications 4:326–337.
957 Simons, Y. B., and G. Sella. 2016. The impact of recent population history on the deleterious
958   mutation load in humans and close evolutionary relatives. Current Opinion in Genetics &
959   Development 41:150–158.
960 Slatyer, R. A., M. Hirst, and J. P. Sexton. 2013. Niche breadth predicts geographical range size: a
961   general ecological pattern. Ecology Letters 16:1104–1114.
962 Smith, J., G. Coop, M. Stephens, and J. Novembre. 2018. Estimating time to the common
963   ancestor for a beneficial allele. Molecular Biology and Evolution 35:1003–1017.
964 Song, Y., S. Endepols, N. Klemann, D. Richter, F.-R. Matuschka, C.-H. Shih, M. W. Nachman,
965   et al. 2011. Adaptive introgression of anticoagulant rodent poison resistance by
966   hybridization between old world mice. Current Biology 21:1296–1301.
967 Stewart, G. S., M. R. Morris, A. B. Genis, M. Szűcs, B. A. Melbourne, S. J. Tavener, and R. A.
968   Hufbauer. 2017. The power of evolutionary rescue is constrained by genetic load.
969   Evolutionary Applications 10:731–741.
970 Stoletzki, N., and A. Eyre-Walker. 2006. Synonymous codon usage in *Escherichia coli*: selection
971   for translational accuracy. Molecular Biology and Evolution 24:374–381.
972 Swenson, N. G., and D. J. Howard. 2005. Clustering of contact zones, hybrid zones, and
973   phylogeographic breaks in North America. The American Naturalist 166:581–591.
974 Taylor, S. A., and E. L. Larson. 2019. Insights from genomes into the evolutionary importance
975   and prevalence of hybridization in nature. Nature Ecology and Evolution. Nature
976   Publishing Group.
977 Teshima, K. M., and M. Przeworski. 2006. Directional positive selection on an allele of arbitrary
978   dominance. Genetics 172:713–8.
979 Turner, J. R. G. 1981. Adaptation and evolution in *Heliconius*: a defense of NeoDarwinism.
980   Annual Review of Ecology and Systematics 12:99–121.
981 Wang, J., and M. C. Whitlock. 2003. Estimating effective population size and migration rates
982   from genetic samples over space and time. Genetics 163:429–446.
983 Waples, R. S. 2015. Testing for Hardy-Weinberg proportions: have we lost the plot? Journal of
984   Heredity 106:1–19.
985 Willi, Y., M. Fracassetti, S. Zoller, and J. Van Buskirk. 2018. Accumulation of mutational load
986   at the edges of a species range. Molecular Biology and Evolution 35:781–791.
987 Wright, S. 1931. Evolution in Mendelian populations. Genetics 16:97–159.
988 Zheng, Y., R. Peng, M. Kuro-o, and X. Zeng. 2011. Exploring patterns and extent of bias in
989   estimating divergence time from mitochondrial DNA sequence data in a particular
990   lineage: a case study of salamanders (Order Caudata). Molecular Biology and Evolution.
991   Narnia.
992 Zimova, M., L. S. Mills, and J. J. Nowak. 2016. High fitness costs of climate change-induced
993   camouflage mismatch. Ecology Letters 19:299–307.
994